Computation of Thermal Condition in an Induction Motor during Direct-On-line Starting

A.K.NASKAR
Department of electrical engineering
Seacom Engineering College
Howrah-711302, India
Email-naskar73@gmail.com
D.SARKAR
Department of electrical engineering
Bengal Engineering & Science University
Shibpur, Howrah-711103, India

Abstract: Induction machines transient thermal analysis has been a subject of interest for machine designers in their effort to improve machine reliability. The stator being static is prone to high temperature and the study of transient thermal behaviour in the stator is useful to identify causes of failure in induction machines. The paper presents a two-dimensional transient heat flow in the stator of an induction motor using arch shaped elements in the r-θ plane of the cylindrical co-ordinate system. The model is applied to one squirrel cage TEFC machine of 7.5 kW. Finally the temperatures obtained by this two-dimensional approximation have been compared for different stator currents considering the time required for each stator current during the transient in direct-on-line starting.

Key words: *FEM, Induction Motor, Thermal Analysis, Transients, Design Performance***.**

1. Introduction

The general heating problems of induction motor and the prediction of temperature rise of magnetic core, insulation, conductors etc. are the problems of determining the three dimensional temperature distribution produced by a system of current carrying conductors, which specify different locations of heat sources. Often three-dimensional heating problems can be reduced to more tractable two-dimensional problems by recognizing some simplifying assumptions that the essential description of the geometry requires only two independent co-ordinates. For these types of problems, we may determine temperatures by studying only a unit thickness of the geometry in the r - θ plane of the cylindrical co-ordinate system.

Most of the earlier designers and researchers have traditionally adopted analytical methods such as separation of variables, conformal mapping, and resistance analog networks for prediction of temperatures. The analytical work is largely limited and that too with many major assumptions. Even though the resistance analog method predicts average temperatures quite accurately, the method failed in predicting hot spot temperatures. Rossenberry Jr.[1] used thermal resistance networks to predict transient stalled temperatures of cast aluminium squirrel cage motors as early as 1955. Mellor et al [2] have presented exhaustive study on lumped parameters thermal model for TEFC machines both under steady and transient thermal conditions.

Finite difference is one of the popular numerical methods widely used. The estimation of core iron and copper winding temperatures in electrical machines, the finite difference method [3], [4] had been normally employed. Even though this method predicts hot spot temperatures, the method is not as flexible as finite element method [12], [13], [15], [16] in handling complex boundary condition and geometry. Use of finite elements for solution of heat flow has wide acceptance among researchers in recent years. Rajagopal et al [9], [10] have carried out two-dimensional steady state and transient thermal analysis of TEFC machines using FEM. The two- dimensional finite element procedure was first introduced in papers by Clough [5], [6].

Use of finite elements has seldom been attempted due to the complexity and high cost of computation and detailed 2-dimensional transient thermal analysis area not known to be reported for direct-on-line starting of induction motors.

In this paper, a finite element solution of the two-dimensional transient heat conduction in cylindrical co-ordinate system with explicitly derived solution matrices is introduced. In the r - θ plane arch shaped finite elements are introduced. The explicit nature of the solution matrices allows for optimal computer usage. The temperature distribution in the r - θ plane has been determined by taking only a strip of unit thickness in the stator bounded by planes at mid-slot, mid-tooth divided into 24 arch shaped elements and thus provides a new approach of multi-time interval solution to a transient stator heating problem and this defines the scope of this technique. The requirements

of computer storage for a large number of elements have been reduced by the use of half bandwidth of the symmetric matrix.

The method is directly applicable to the study of temperature rise during direct-on-line starting that may arise following some intentional starting action. The procedure is particularly suited to the study of transient heating of the stator coils due to I^2R losses in the coil slots during starting action .The direct on line starting method is the most simple and inexpensive method of starting a squirrel cage induction motor.

2. Formulation of the Problem

The formulation of the transient heat conduction problem for finite element analysis follows a weighted residual approach. The steps taken in the formulation are as follows:

(a) Formulate the transient heat conduction equation in cylindrical polar co-ordinates.
(b) Specify interpolation polynomials (shape functions) for the element in such a way that the element equations can be directly integrated.
(c) Deduce finite-element equations directly from the governing differential equation of the problem without any classical, quasi-variational or restricted variational principles.
(d) Solve the set of algebraic linear equations at each instant in time by Gauss method, which takes advantage of the symmetric banded nature of the matrices.

3. Transient Heat-conduction

The general form of the heat conduction equation is

$$q = - V \nabla T \qquad \ldots. (1)$$

T is the potential function (Temperature) ^oC.
V is the medium permeability (Thermal conductivity) watt /m ^oC
q is the flux (heat flux) watt / m^2 .

For a solid in which heat is being generated internally at rate Q watt / m^3, consideration of conservation of energy produces the general transient heat conduction equation

$$V \nabla^2 T = P_m C_m \frac{\delta T}{\delta t} - Q \qquad .. (2)$$

Where, P_m, C_m are the material density and specific heat.

In cylindrical polar co-ordinates, equation (2) can be expanded as

$$\frac{1}{r} \frac{\delta}{\delta r} \left(V_r \, r \frac{\delta T}{\delta r} \right) + \frac{V_\theta}{r^2} \frac{\delta^2 T}{\delta \theta^2} + Q - P_m \, C_m \frac{\delta T}{\delta t} = 0 \qquad .. (3)$$

V_r, V_θ are thermal conductivities in the radial, circumferential directions respectively.

4. Finite Element Equations (The Galerkin Method)

The solution of equation (3) can be obtained by assuming the general functional behaviour of the dependent field variable in some way so as to approximately satisfy the given differential equation and boundary conditions. Substitution of this approximation into the original differential equation and boundary conditions then results in some error called a residual. This residual is required to vanish in some average sense over the entire solution domain.

The approximate behaviour of the potential function within each elements is prescribed in terms of their nodal values and some weighting functions N_1 , N_2 … such that

$$T = \sum_{i = 1, 2 \ldots m} N_i \, T_i \qquad \ldots.(4)$$

The weighting functions are strictly functions of the geometry and are termed shape functions. These shape functions determine the order of the approximating polynomials for the heat conduction problem.

The weighting functions are strictly functions of the geometry and are termed shape functions. These shape functions determine the order of the approximating polynomials for the heat conduction problem.

The method of weighted residuals determines the 'm' unknowns T_i in such a way that the error over the entire solution domain is small. This is accomplished by forming a weighted average of the error and specifying that this weighted average vanish over the solution domain.

The required equation governing the behaviour of an element is given by the following expression:

$$\iint_{D^{(e)}} N_i \left[\frac{\delta}{\delta r} \left(V_r \frac{\delta T^{(e)}}{\delta r} \right) + \frac{\delta}{\delta \theta} \left(\frac{V_\theta}{r^2} \frac{\delta T^{(e)}}{\delta \theta} \right) + Q - P_m \, C_m \frac{\delta T^{(e)}}{\delta t} \right] r \, d\theta \, dr = 0 \qquad .. (5)$$

Equation (5) can be written as

$$\iint_{D^{(e)}} N_i \left[\frac{\delta}{\delta r} \left(V_r \frac{\delta T^{(e)}}{\delta r} \right) + \frac{\delta}{\delta \theta} \left(\frac{V_\theta}{r^2} \frac{\delta T^{(e)}}{\delta \theta} \right) + Q - P_m \, C_m \frac{(2T^{(e)} - 2T_o^{(e)})}{2\Delta t} \right] r \, d\theta \, dr = 0 \qquad \ldots(6)$$

Where T_o is the temperature at the previous point in time and Δt is the time interval.

Equation (6) expresses the desired averaging to the error or residual within the element boundaries, but it does not admit the influence of the boundary. Since we have made no attempt to choose the N_i so as to satisfy the boundary conditions, we must use integration by parts to introduce the influence of the natural boundary conditions.

4.1. Arch-Element Shape Functions

Consider the arch-shaped prism element of Fig. 1 formed by circle arcs radii a, b, radii inclined at an angle 2α.

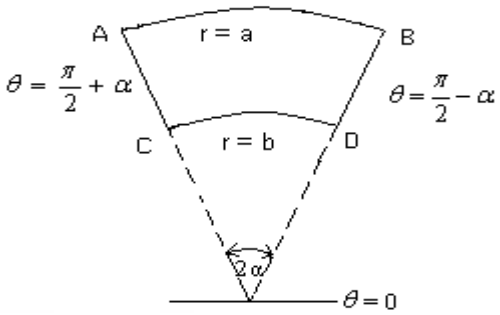

Fig.1. Two-dimensional arch-shaped prism element suitable for discretisation of induction motor stator.

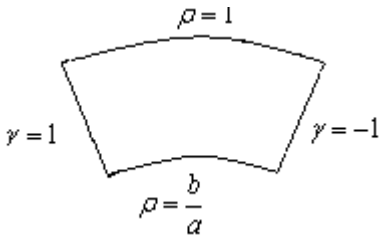

Fig.2. The non-dimensional arch element

The shape functions can be defined in terms of a set of non-dimensional co-ordinates by non-dimensionalizing the cylindrical polar co-ordinates r, θ, using

$$\rho = \frac{r}{a}; \quad \vartheta = \frac{\theta - \frac{\pi}{2}}{\alpha}$$

The arch element with non-dimensional co-ordinates is shown in Fig. 2.

The temperature at any point within the element be given in terms of its nodal temperatures by

$$T = T_A N_A + T_B N_B + T_C N_C + T_D N_D \quad .. (7)$$

Where the N's are shape functions chosen as follows:

$$N_A = \frac{\left(\rho - \frac{b}{a}\right)(\vartheta - 1)}{-2\left(1 - \frac{b}{a}\right)}; \qquad N_C = \frac{(\rho - 1)(\vartheta + 1)}{-2\left(1 - \frac{b}{a}\right)}$$

$$N_B = \frac{\left(\rho - \frac{b}{a}\right)(\vartheta + 1)}{2\left(1 - \frac{b}{a}\right)}; \qquad N_D = \frac{(\rho - 1)(\vartheta - 1)}{2\left(1 - \frac{b}{a}\right)} \ldots (8)$$

It is seen that the shape functions satisfy the following conditions

(a) That at any given vertex 'A' the corresponding shape function N_A has a value of unity and the other shape functions N_B , N_C have a zero value at this vertex. Thus at node j, $N_j = 1$ but $N_i = 0$, $i \neq j$.

(b) The value of the potential varies linearly between any two adjacent nodes on the element edges.

(c) The value of the potential function in each element is determined by the order of the finite element. The order of the element is the order of polynomial of the spatial co-ordinates which describes the potential within the element. The potential varies as a quadratic function of the spatial co-ordinates on the faces and within the element.

4.2. Boundary Conditions

The details of the induction motor are shown in Figure 3. In this analysis, the two-dimensional domain of core iron and winding chosen for modeling the problem and the geometry is bounded by planes passing through the mid-tooth and the mid-slot. This is shown in Fig.4, taken from the shaded region A of Fig 3. The temperature distribution is assumed symmetrical across these two planes, with the heat flux normal to the two surfaces being zero. From the other two boundary surfaces, heat is transferred by convection to the surrounding gas. It is convected to the air-gap gas from the teeth, to the back of core gas from the yoke iron.

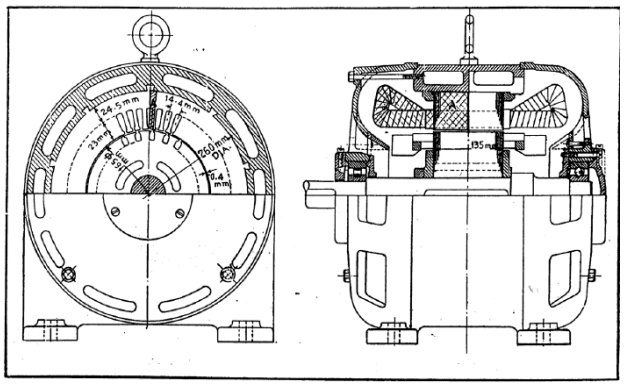

Fig.3. Half sectional end & sectional elevation of a 7.5 kW squirrel cage induction motor

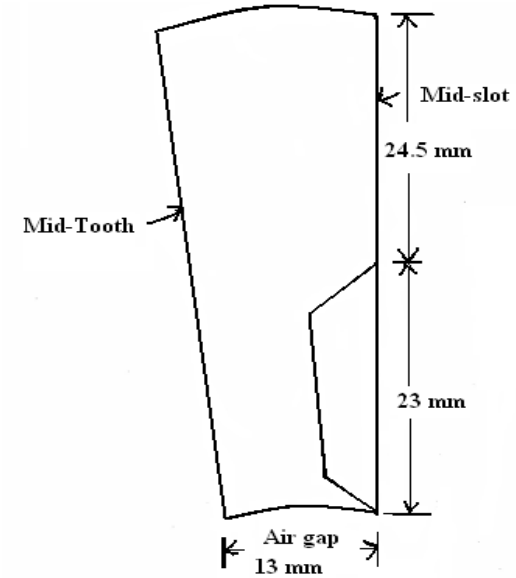

Fig. 4. Slice of core iron & winding bounded by planes at mid-slot, mid-tooth.

The boundary conditions may be written in terms of $\delta T / \delta n$, the temperature gradient normal to the surface.

Mid-slot surface $\dfrac{\delta T}{\delta n_S} = 0$ .. (9)

Mid-tooth surface $\dfrac{\delta T}{\delta n_t} = 0$ .. (10)

Air-gap surface $h\left(T - T_{AG}\right) = - V_r \dfrac{\delta T}{\delta n_{AG}}$ .. (11)

Where, T= Surface temperature and T_{AG}= Air-gap gas temperature

Back-of-core surface, $h\left(T - T_{BC}\right) = - V_r \dfrac{\delta T}{\delta n_{BC}}$ .. (12) T_{BC} = Back of core gas temperature.

5. Approximate Numeric Form

The heat flow equation may be formulated in Galerkin's form, the solution being obtained by specializing the general functional form to a particular function, which then becomes the approximate solution sought.

using our attention on equation (6), we obtain through integration by parts

$$\iint_{D^{(e)}} N_i \frac{\delta}{\delta r}\left(V_r \frac{\delta T^{(e)}}{\delta r}\right) r\, d\theta\, dr = \int_{S_2^{(E)}} V_r \frac{\delta T^{(e)}}{\delta r} N_i\, r\, d\theta - \iint_{r,\theta} V_r \frac{\delta T^{(e)}}{\delta r}\frac{\delta N_i}{\delta r} r\, d\theta\, dr$$

$$= \int_{S_2^{(E)}} V_r \frac{\delta T^{(e)}}{\delta r} n_r\, N_i\, d\sum - \iint_{r,\theta} V_r \frac{\delta T^{(e)}}{\delta r} \cdot \frac{\delta N_i}{\delta r} r\, d\theta\, dr \quad \ldots(13)$$

Where n_r is the r component of the unit normal to the boundary and $d\Sigma$ is a differential arc length along the boundary.

Equation (6) takes the form

$$- \iint_{D^{(e)}} \left(V_r \frac{\delta T^{(e)}}{\delta r}\frac{\delta N_i}{\delta r} + \frac{1}{r^2} V_\theta \frac{\delta T^{(e)}}{\delta \theta}\frac{\delta N_i}{\delta \theta}\right) r\, d\theta\, dr + \iint_{D^{(e)}} (N_i Q)\, r\, d\theta\, dr$$

$$- \iint_{D^{(e)}} \frac{P_m C_m}{2\Delta t}\left(2T^{(e)} N_i - 2T_o N_i\right) r\, dr\, d\theta$$

$$+ \int_{S_2^{(e)}} \left(V_r \frac{\delta T^{(e)}}{\delta r} n_r + \frac{1}{r^2} V_\theta \frac{\delta T^{(e)}}{\delta \theta} n_\theta \right) N_i\, d\sum^{(e)} = 0$$

for i = A, B, C, D .. (14)

The surface integral (boundary residual) in equation (14) now enables us to introduce the natural boundary conditions of equations (9 – 12).

Equation (14) can be written with respect to the nodal temperatures as

$$0 = \iint_{r,\theta} \left[V_r \frac{\delta T^{(e)}}{\delta r}\frac{\delta}{\delta r}\left(\frac{\delta T^{(e)}}{\delta r}\right) + \frac{V_\theta}{r^2}\frac{\delta T^{(e)}}{\delta \theta}\frac{\delta}{\delta \theta}\left(\frac{\delta T^{(e)}}{\delta \theta}\right) - Q N_i \right] r\, dr\, d\theta + \int_{S_2^{(e)}} h\left(N\right)\left(T^{(e)}\right) N_i\, d\sum^{(e)}$$

$$+ \frac{P_m C_m}{2\Delta t} \iint_{r,\theta} \left[2\left[N\right]\left\{T\right\} N_i - 2T_o N_i \right] r\, dr\, d\theta$$

for i = A, B, C, D .. (15)

There are four such equations as (15) for the four vertices of the element.

These equations, when evaluated lead to the matrix equation

$$\left[\left[S_R\right] + \left[S_\theta\right] + \left[S_T\right] + \left[S_H\right]\right]\left[T\right] = \left[S_T\right]\left[T_O\right] + \left[R\right] + \left[S_C\right] \quad .. (16)$$

$[S_R]$, $[S_\theta]$ are symmetric co-efficient matrices.

$[S_T]$ is the heat capacity matrix.

$[S_H]$ is the heat convection matrix.

[T] is the column vector of unknown temperatures.

[R] is the forcing function (heat source) vector.

$[S_C]$ is the column vector of heat convection.

$[T_o]$ is the column vector of unknown (previous point in time) temperatures.

The explicit derivation of $\left[S_R\right], \left[S_\theta\right], \left[S_T\right]$ & $\left[R\right]$ matrices of equation (16) is given in the appendix.

6. Method of Solution

The system of global equations, as determined by equation (16), has to be solved to determine the nodal temperatures.

The solution of this set of linear simultaneous equations is determined by the Gauss method [8], which takes the advantage of the banded nature of the matrices. To save computer memory, the symmetric matrix is half bandwidth, efficiently stored by Gauss

routine, by which extremely large problems can be effectively solved.

7. Application to a Polyphase Induction Motor

The problem concerns heat flow through core iron and winding in the stator of an induction motor. The stator being static is prone to high temperature and the temperature distribution of the stator only is computed here. The hottest spot is generally in the copper coils. The heat from the outer surfaces, i.e., the back of core surface and the air-gap surface is lost through convective mode of heat transfer. Thermal conductivity of copper and insulation in the slot are taken together for simplification of calculations [11], [14].

As the temperature is maximum at the central plane, the temperature distribution in the plane can be determined approximately by taking this as a two-dimensional r-θ problem with the following assumptions.

(a) The temperature in the strip of unit thickness on the central axis is assumed to be fixed axially i.e. no axial flow of heat is assumed in the central plane. This assumption is permissible because in the central plane where the temperature distribution is maximum, the temperature gradient in the axial direction is zero.

(b) The convection is taken care of only at the cylindrical surfaces neglecting the convection at the end surfaces. Because of this assumption, the temperatures calculated in the central plane will be slightly higher than the actual.

In the case of transient stator heating caused by direct-on-line starting, the transient analysis procedure is able to provide an estimate of the temperatures throughout the volume of the stator at an interval of time required to bring the motor from rest to rated speed by providing rated voltage and current required by the induction motor during the starting action.

Assuming that the motor is at rest with its stator winding at normal ambient temperature, rated voltage and current are injected to the stator winding of the machine. The temperatures within the volume of the stator are calculated at all nodal points for a period of the time required for starting action.

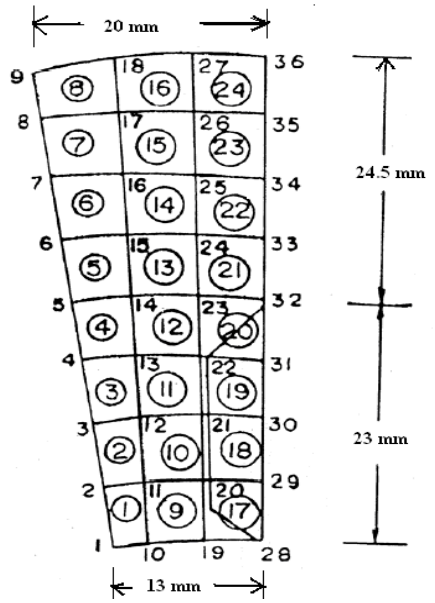

Fig. 5. Slice of core iron & winding bounded by planes of mid-slot & mid-tooth divided into arch shaped Finite Elements.

In this analysis because of symmetry the two-dimensional domain in cylindrical polar co-ordinate of core iron and winding, chosen for modeling the problem and the geometry is bounded by planes passing through the mid-tooth and the mid-slot, which are divided into finite elements as shown in Fig 5. Arch-shaped elements are used throughout the solution region.

7.1 Convective Heat Transfer Co-efficient [7, 9]

Two separate values of convective heat transfer co-efficient have been taken for the cylindrical curved surface over the stator frame and the cylindrical air gap surface.

The natural convection heat transfer co-efficient on cylindrical curved surface over the stator frame are dependent on Grashof number (G_r) and Prandtl number (P_r) according to the following equation :

$$h = \frac{0.53 \times (G_r \, P_r)^{1/4} \times K}{d}$$

Where, d = hydraulic diameter = 0.26 m
and K=fluid thermal conductivity = 0.0297386 W / m^{o}C

$$\text{The Grashof number} = G_r = \frac{g\beta (T_W - T_\infty) \times d^3}{V^2}$$

Where, g = 9.8 m / s^2

$$\beta = \frac{1}{T_f} = \frac{1}{345.5} = 2.89 \times 10^{-3} \ K^{-1}$$

And V = Kinematic viscosity = 20.03 x 10^{-6} m^2 / sec.

G_r = 80648337.

The Prandtl number $= P_r = \frac{C_P \mu}{K}$

Where, C_P = Fluid specific heat = 1008.344 J / kg ^oC and μ = Fluid dynamic viscosity = 2.06 x 10^{-5} kg / m-s

P_r = 0.698.

By calculation, h = 5.25 W / m^2 ^oC

The heat transfer co-efficient on forced convection for turbulent flow in cylindrical air-gap surface are dependent on the Reynolds number (R_e) and the Prandtl number (P_r) according to the following equation :

$$h = \frac{0.026 \times (R_e)^{0.805} \times (P_r)^{1/3} \times K}{d}$$

Where, K = Fluid thermal conductivity = 0.0297386 W / m ^oC

And d = Hydraulic diameter = 0.165 m.

The properties of air are evaluated at film temperature with the maximum permissible temperature assumed to be 105 ^oC and an ambient temperature assumed to be 40^oC.

The Reynolds number $= R_e = \frac{PVd}{\mu}$

Where, p = Fluid density = 1.022 kg / m^3

V = Fluid velocity = 17.5 m / s

μ = Fluid viscosity = 2.06 x 10 kg / m – s

R = 143253.64

The Prandtl number $= P_r = \frac{C_P \mu}{K}$

Where, C_P = Fluid specific heat = 1008.344 J / kg ^oC

P_r = 0.698.

By calculation, h = 60.16 W / m^2 ^oC .

The velocity and Reynold's number in the air-gap are functions of rotor peripheral speed, stator roughness and air-gap width.

7.2. Thermal Constants [9]

For a transient problem in two dimensions, the following properties are required for each different material:

(a) Thermal conductivity, radial direction, V_r, watt /m ^oC

(b) Thermal conductivity, circumferential direction, $V_\circ$,watt / m ^oC

(c) Material density, P_m, kg / m^3.

(d) Material specific heat, C_m, watt Sec / kg ^oC

The thermal conductivity, material density, material specific heat for different materials of induction motor stator is given in Table-1.

Table.1

Typical set of material properties of induction motor stator

	Magnetic Steel Wedge	Copper and Insulation
V_r	33.07	2.007
$V_\circ$	0.826	1.062
P_m	7.8612	8.9684
C_m	523.589	385.361

7.3 Calculation of Heat losses

Heat losses in the tooth and yoke of the core are based on calculated magnetic flux densities (0.97 wb / m^2 and 1.293 wb / m^2, respectively) in these regions. Tooth flux lines are predominantly radial and yoke flux lines are predominantly circumferential. The grain orientation of the core punching differs in these two directions and therefore influences the heating for a given flux density. Copper losses in the winding are determined from the length as well as the area required for the conductors in the slot.

Diameter of stator bore D = 165 mm;

Stator core length L = 140 mm;

Pole pitch $Y = \frac{\pi D}{P} = \pi \times \frac{165}{4} = 129.6 \text{ mm};$

And flux per pole

$$\varphi_m = \bar{B} Y L = 0.45 \times \frac{129.6}{1000} \times \frac{140}{1000} \times 1000 \text{ mwb} = 8.16 \text{ mwb}.$$

Stator Core

Stator core depth = 24.5 mm, Stator slot depth = 23 mm

Mean diameter = 165 + 2 × slot depth + stator core depth = 165 + 46 + 24.5 = 235.5 mm.

Area of core =

$$\frac{1/2 \times \phi_m}{B_C} = \frac{1/2 \times 8.16 \times 10^{-3}}{1.293} = 3.15545 \times 10^{-3} \text{ m}^2 = 3155.45 \text{ mm}^2$$

Volume of core

$= 3155.45 \times \pi \times 235.5 = 2334544.1 \text{ mm}^3$

Iron loss in stator core = 90.75 W

Iron loss in stator core per unit volume

$$= \frac{90.75}{2334544.1} = 3.88708 \times 10^{-5} \text{ W/mm}^3.$$

Stator Teeth

Width of tooth = 7.5 mm
Number of tooth in the stator = 36
Taking iron factor = 0.9
Net core length of stator = 0.9 × 140 = 126 mm
Area of one tooth = width of tooth × net iron length of stator = 7.5 × 126 mm = 945 mm^2
Total area of all teeth = 945 × 36 mm^2 = 34020 mm^2
Volume of teeth = 945 × 36 × slot depth or tooth height

$$= 945 \times 36 \times 23\ mm^2 = 782460\ mm^3$$

Iron loss in stator teeth = 30.7 W
Iron loss in stator teeth per unit volume

$$= \frac{30.7}{782460} = 3.92352 \times 10^{-5}\ W/mm^3$$

Stator Copper

The term Direct-On-Line starting as applied to the induction motor refers to the system of starting method in which the stator windings of the motor is excited by rated voltage under D.O.L starting conditions, an induction motor usually requires approximately 6 times its rated current when the rated voltage as applied to the stator.
Referring the equivalent circuit of fig. 6

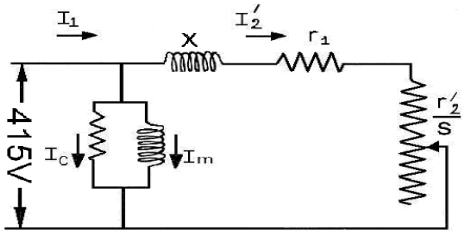

Fig. 6. Equivalent circuit on induction motor.

x_1=8.15Ω ; I_c=0.176 Amp; r_1=2.04Ω; I_m= 2.41Amp
$r_2^{/} = 2.39\Omega$; $V_1 = 415\ V$;
Electromagnetic torque,

$$T_e = \frac{3}{\omega_S} E_t^{\,2} \frac{r_2'/s}{\left(r_1 + r_2'/s\right)^2 + \left(X_1 + X_2'\right)^2}$$

Stator current, $I_1 = \sqrt{\dfrac{T_e \omega_S}{3\dfrac{r_2^{/}}{s}}}$

Starting condition of the motor are those for S=1

At starting, S=1

$$T_e = \frac{3}{50\pi}(415)^2 \frac{2.39/1}{(2.04 + 2.39/1)^2 + (8.15)^2}$$

$$= 91.3575\ N.m$$

$$I_1 = \sqrt{\frac{91.3575 \times 50\pi}{3 \times 2.39}} = 44.737A.$$

Since the starting conditions of the motor are those for S=1 to S=0.04, the starting current per phase at start i.e, at S=1 is 44.737 Amp and at full load slip S=0.04 is 6.658Amp.

At full load slip, S=0.04

$$T_e = \frac{3}{50\pi}(415)^2 \frac{2.39/0.04}{(2.04 + 2.39/0.04)^2 + (8.15)^2}$$

$$= 50.5935\ N.m$$

$$I_1 = \sqrt{\frac{50.5935 \times 50\pi}{3 \times 2.39/0.04}} = 6.658\ Amp.$$

In order to obtain physically operation in the region of slip 0.04<S<1, the current distributions during D.O.L starting condition is calculated using detailed equivalent circuit of the machine.

At S=0.8, the starting current = 43.336 Amp
At S=0.6, the starting current = 40.950 Amp
At S=0.4, the starting current = 36.304 Amp
At S=0.2, the starting current = 25.631 Amp
At S=0.08, the starting current = 12.598 Amp
At S=0.06, the starting current = 9.728 Amp
At S=0.04, the starting current = 6.658 Amp

Stator Copper Loss during Transient at different Slips

Copper loss at different slips is calculated as below:
No. of slot = 36
Volume of copper = 92mm x 409 mm^2 = 37628mm^3
$r_{1=}$2.04
Stator copper loss = $3I_1^2 r_1$ / No. of slots
At s =1
Stator copper loss per slot =
$(3 \times (44.73)^2 \times 2.04)/36$= 340.131watt
Stator copper loss per slot per unit volume = stator copper loss per slot/ volume of copper = 340.131/37,628 = 0.009039 watt/mm^3

Assuming a load of moment of inertia 10 kg-m^2, the time required is calculated at different intervals of speed, i.e., from rest, S=1 to S=0.8 as 3.185 sec to accelerate the motor at a speed of 1440 rpm i.e., 0.96

of the synchronous speed from rest by direct on line starting. The computation of different parameters for starting at different slips in direct-on-line mode is shown in Table- 2.

Table.2.

The different values of stator currents, stator coppers loss/slot/unit volume, electromagnetic torque T_e and time required for starting action at different slips in direct-on-line starting.

Slip	Current (Amp)	Electro-magnetic torque T_e(N.m)	Stator copper loss /slot/unit volume (W/mm^3)	Time t_s (sec)	Time t_s (sec)
1	44.73	91.3575	0.009039	0.0	3.185
0.8	43.336	107.157	0.008485	3.185	2.689
0.6	40.95	127.569	0.007576	5.874	2.271
0.4	36.304	150.406	0.005955	8.145	2.033
0.2	25.631	149.938	0.002968	10.178	1.524
0.08	12.598	90.566	0.000717	11.702	0.398
0.06	9.728	71.995	0.000428	12.091	0.516
0.04	6.658	50.593	0.000200	12.607	

Solutions are done for the two-dimensional structure first with maximum permissible temperature and then calculating the heat transfer co-efficient at the mean of the two temperatures as tabulated below in table-3. The temperatures obtained are found to be within the permissible limit in terms of overall temperature rise under transient condition.

Since the temperature evolution in hottest spots is obviously the stator copper, temperature variation with time at crucial points has been depicted in graphs as shown in figures 10-15.

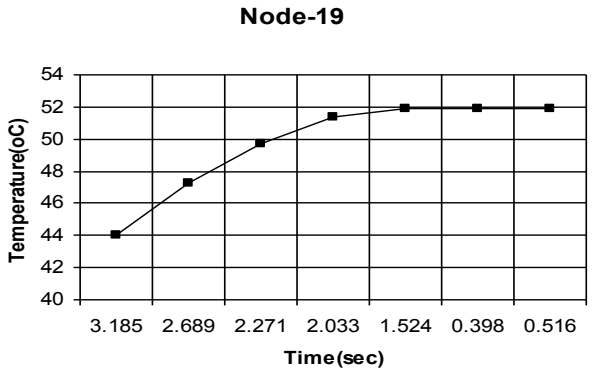

Fig.7. Temperature variation with time

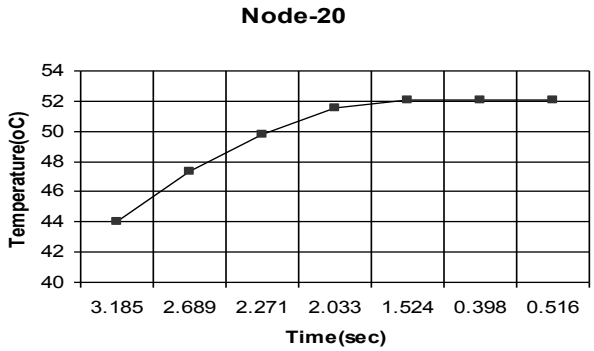

Fig.8. Temperature variation with time

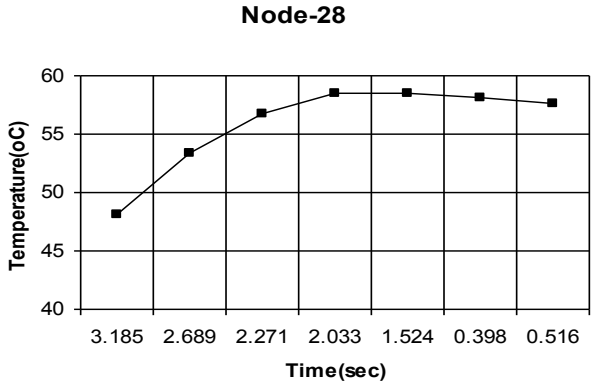

Fig.9. Temperature variation with time

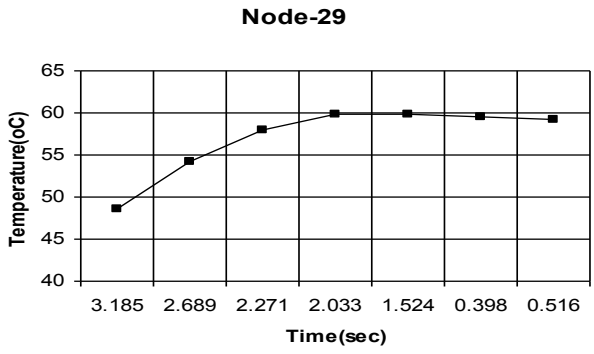

Fig.10. Temperature variation with time

Table.3: Solutions are done for the two-dimensional structure

Node Numbers	Initial Temperatures	CORRESPONDING TEMPERATURES FOR DIFFERENT STATOR CURRENTS DURING DIRECT-ON-LINE STARTING						
		Q=0.009039	Q=0.008485	Q=0.007576	Q=0.005955	Q=0.002968	Q=0.000717	Q=0.000428
		I_1=44.737 Amp Starting time=3.185 sec	I_1=43.336 Amp Starting time=2.689 sec	I_1=40.949 Amp Starting time=2.271sec	I_1=36.304 Amp Starting time=2.033 sec	I_1=25.631 Amp Starting time=1.524 sec	I_1=12.598 Amp Starting time=0.398 sec	I_1=9.728 Amp Starting time=0.516 sec
19	40°C	44.021°C	47.273°C	49.692°C	51.337°C	51.889°C	51.910°C	51.902°C
20	40°C	44.056°C	47.359°C	49.826°C	51.510°C	52.071°C	52.096°C	52.094°C
21	40°C	44.022°C	47.269°C	49.663°C	51.267°C	51.750°C	51.758°C	51.733°C
22	40°C	43.696°C	46.431°C	48.351°C	49.557°C	49.802°C	49.737°C	49.637°C
23	40°C	41.576°C	42.835°C	43.788°C	44.455°C	44.694°C	44.708°C	44.718°C
24	40°C	40.414°C	40.965°C	41.480°C	41.929°C	42.224°C	42.299°C	42.383°C
28	40°C	48.116°C	53.421°C	56.780°C	58.561°C	58.439°C	58.112°C	57.670°C
29	40°C	48.544°C	54.242°C	57.909°C	59.919°C	59.903°C	59.593°C	59.166°C
30	40°C	48.424°C	54.254°C	58.113°C	60.311°C	60.460°C	60.198°C	59.823°C
31	40°C	50.038°C	56.491°C	60.370°C	62.223°C	61.746°C	61.012°C	60.360°C
32	40°C	42.122°C	43.267°C	43.937°C	44.249°C	44.112°C	43.976°C	43.831°C
33	40°C	40.576°C	41.251°C	41.802°C	42.229°C	42.466°C	42.513°C	42.566°C

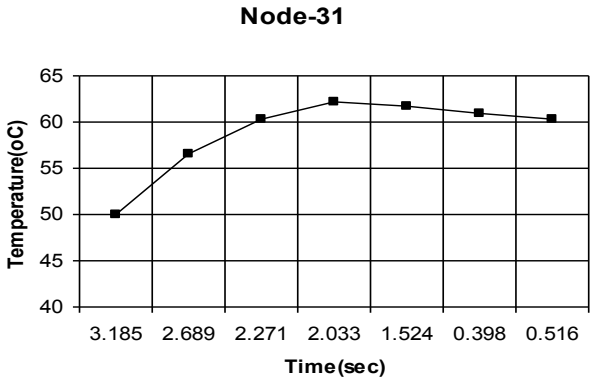

Fig.11. Temperature variation with time

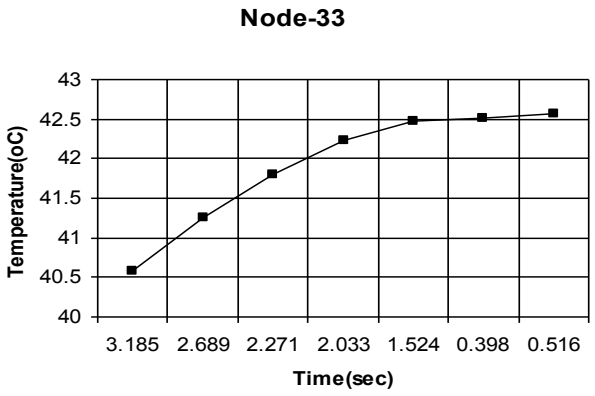

Fig.12. Temperature variation with time

8. Data Analysis

Since the hottest spots are found to be in the stator copper as envisaged from the calculated temperatures for the two-dimensional structure during the D.O.L starting period the temperature variation with time in each node of copper is taken as an index to understand the temperature profile during the transient. It is to be noted that the temperature is found to be maximum at the nodes pertaining to copper in the axis of symmetry.

As a consequence, the temperature variation with time at hottest spots has been depicted in graphs as shown in fig.7-12 to compare the magnitude of the maximum temperature variation with time at different nodal points along the stator copper winding.

9. Conclusion

The two-dimensional transient finite element procedure for the thermal analysis of large induction-motor stators provides the opportunity for the in-depth studies of stator heating problems. By virtue of the new, explicitly derived arch element, together with an efficient bandwidth and Gauss routine, extremely large problems can be efficiently solved.

A new two-dimensional finite element procedure in cylindrical polar co-ordinates, with explicitly derived solution matrices, has been applied to the solution of the transient heat conduction equation during direct-

on-line starting. Though the results are approximate, the method is fast, inexpensive and leads itself to immediate visual pictures of the temperature pattern in a two-dimensional slice of iron core and winding in the stator of an induction motor.

References

1. Rosenberry,G.M.Jr., "The transient stalled temperature rise of cast aluminium squirrel case rotors for induction motors", *AIEE Trans*.Vol.PAS 7,1955.
2. Mellor, P.H., Roberts, D.R., and Tumer,D.R., "Lumped parameter thermal model for electrical machines of TEFC design",*IEE Proceedings B*, Vol.138, September 1971.
3. Reichert, K., "The calculation of the temperature distribution in electrical machines with the aid of the finite difference method",*EGZ. A Bd.* 90, H6, pp.137-142 , 1969.
4. Williamson,S.,and Walker,J.D., "Calculation of stall bar temperature rise",*5th Int.Conf. on electrical machines and drives*, 11-13 Sept, 1991.
5. Clough, R.W., "The finite element in plane stress analysis," *Proc. 2nd A.S.C.E. Conf on Electronic Computation*, Pittsburgh,Pa., Sept.1960.
6. Turner, M.J.,.Clough, R.W.,.Martin, H.C., and.Topp, L.J., "Stiffness and deflection analysis of complex structures", *J.Aero.Sci*.,23, 805-23,1956.
7. Armor, A.F., and Chari, M. V. K., "Heat flow in the stator core of large turbine generators by the method of three-dimensional finite elements, Part-I: Analysis by Scalar potential formulation: Part - II: Temperature distribution in the stator iron," *IEEE Trans,* Vol. PAS-95, No. 5, pp.1648-1668, September 1976.
8. Sarkar, D., Mukherjee, P,K., Sen, S,K., "Approximate Analysis of Steady State Heat conduction In An Induction Motor" *IEEE Transactions on Energy Conversion*, Vol. 8, No.1, pp. 78 – 84, March 1993.
9. Rajagopal,M.S.,Kulkarni,D.B.,Seetharamu,K.N., and Ashwathnarayana P.A.,"Axi-symmetric steady state thermal analysis of totally enclosed fan cooled induction motors using FEM", *2nd Nat Conf.on CAD/CAM*,19-20 Aug,1994.
10. Rajagopal, M.S.,Seetharamu, K.N.and shwathnarayana. P.A.,"Transient thermal analysis of induction motors", IEEE Trans on Energy conversion, Vol.13, No.1, March 1998.
11. Sarkar, D., Naskar, A.K., "Approximate analysis of transient heat conduction in an induction motor during reactor starting", in Proc. IEEE Power Electronics India International Conference (IICPE 2010), Jan, 2011, PP.1-8.
12. Armor, A. F., "Transient Three Dimensional Finite Element Analysis of Heat Flow in Turbine-Generator Rotors", *IEEE Transactions on Power Apparatus and Systems*, Vol. PAS 99, No.3 May/June. 1980.
13. Islam J., Pippuri J., Perho J., Arkkio A., "Time-harmonic finite-element analysis of eddy currents in the form-wound stator winding of a cage induction motor", *IET Electric Power Applications* 1 (2007) 5, pp. 839– 846.
14. D.Sarkar, N.K.Bhattacharya, "Approximate analysis of transient heat conduction in an induction motor during star-delta starting" in Proc. *IEEE Int. Conf. on industrial technology* (ICIT 2006), Dec., PP.1601-1606.
15. E. Dlala, "Comparison of models for estimating magnetic core losses in electrical machines using the finite-element method", *IEEE Transactions on Magnetics*, 45(2):716-725, Feb. 2009.
16. C. Mejuto, M. Mueller, M. Shanel, A. Mebarki, and D. Staton, "Thermal modelling investigation of heat paths due to iron losses in synchronous machines", in *Proc. IEEE PEMD*, Apr. 2008, pp. 225–229.

Appendix

Explicit derivation of the solution matrices:

Equation (15) represents four finite element equations, which involve integration over the domain of the arch element, so that no numerical integration is required by the computer. The first term of the integration is (for vertex A).

$$\int_{D^{(e)}} V_r \frac{\delta T}{\delta r} \frac{\delta}{\delta T_A} \frac{\delta T}{\delta r} r\,dr\,d\theta$$

Referring to equation (7) , we see that

$$\int_{D^{(e)}} V_r \frac{\delta T}{\delta r} \frac{\delta}{\delta T_A} \frac{\delta T}{\delta r} r\,dr\,d\theta$$

Referring to equation (7) , we see that

$$\frac{\delta T}{\delta r} = \left[\frac{\delta N_A}{\delta r} \quad \frac{\delta N_B}{\delta r} \quad \frac{\delta N_C}{\delta r} \quad \frac{\delta N_D}{\delta r}\right] \{T\} = T_A \frac{\delta N_A}{\delta r} + T_B \frac{\delta N_B}{\delta r} + T_C \frac{\delta N_C}{\delta r} + T_D \frac{\delta N_D}{\delta r}$$

and $$\frac{\delta}{\delta T_A}\left(\frac{\delta T}{\delta r}\right) = \frac{\delta N_A}{\delta r}$$

Based on the shape functions in equation (8), and noting that $\frac{\delta}{\delta r} = \frac{1}{a}\frac{\delta}{\delta \rho}$; $\frac{\delta}{\delta \theta} = \frac{1}{\alpha}\frac{\delta}{\delta \nu}$

We can deduce that

$$\frac{\delta T}{\delta r}\frac{\delta}{\delta T_A}\left(\frac{\delta T}{\delta r}\right) = T_A \frac{\left(v^2-1\right)}{\left(4a^2q^2\right)} + T_B \frac{(v-1)^2}{\left(-4a^2q^2\right)} + T_C \frac{\left(v^2-1\right)}{\left(4a^2q^2\right)} + T_D \frac{(v-1)^2}{\left(-4a^2q^2\right)}$$

And in the same way

$$\frac{1}{r^2}\frac{\delta T}{\delta\theta}\frac{\delta}{\delta T_A}\left(\frac{\delta T}{\delta\theta}\right)=\frac{T_A}{a^2\rho^2}\frac{\left(\rho-\frac{b}{a}\right)^2}{\left(4a^2q^2\right)}+\frac{T_B}{a^2\rho^2}\frac{\left(\rho-\frac{b}{a}\right)^2}{\left(-4a^2q^2\right)}$$

$$+\frac{T_C}{a^2\rho^2}\frac{(\rho-1)\left(\rho-\frac{b}{a}\right)}{\left(4a^2q^2\right)}+\frac{T_D}{a^2\rho^2}\frac{(\rho-1)\left(\rho-\frac{b}{a}\right)}{\left(-4a^2\rho^2\right)}$$

Where $q=1-\frac{b}{a}$; note that in cylindrical polar

$$dA=dr\,(rd\theta)=a\rho\left(ad\rho\right)\left(\alpha dv\right)=a^2\,\alpha\rho d\,\rho dv$$

Now performing the integration, term by term,

$$\int_{D^{(e)}}\left[V_r\frac{(v-1)^2}{\left(4a^2q^2\right)}\right]\left(a^2\,\alpha\rho d\rho dv\right)=\frac{V_r\alpha}{6q^2}\left(1-\frac{b^2}{a^2}\right)\times 2$$

$$\int_{D^{(e)}}\left[\frac{V_\theta}{a^2\rho^2}\frac{\left(\rho-\frac{b}{a}\right)^2}{\left(4\alpha^2q^2\right)}\right]\left(a^2\,\alpha\rho d\rho\,d\,v\right)=\frac{V_\theta}{4\,\alpha q^2}[A]$$

$$=\frac{V_\theta}{4\,\alpha\,q^2}\int_{b/a}^{1}\frac{\rho\left(\rho-\frac{b}{a}\right)^2}{\rho^2}d\rho\int_{-1}^{1}dv=\frac{V_\theta}{4\,\alpha q^2}[A]$$

$$\left[S_R\right]=\frac{V_r\,\alpha}{6q^2}\left(1-\frac{b^2}{a^2}\right)\begin{bmatrix}2 & 1 & -1 & -2\\ & 2 & -2 & -1\\ \text{SYM} & & 2 & 1\\ & & & 2\end{bmatrix}$$

$$\left[S_\theta\right]=\frac{V_\theta}{4\,\alpha\,q^2}\begin{bmatrix}A & -A & B & -B\\ & A & -B & B\\ \text{SYM} & & C & -C\\ & & & C\end{bmatrix}$$

Where, $A=1-4\frac{b}{a}+3\frac{b^2}{a^2}-2\frac{b^2}{a^2}\log_e\frac{b}{a}$

$$B=-1+\frac{b^2}{a^2}-2\frac{b}{a}\log_e\frac{b}{a}$$

$$C=-3+4\frac{b}{a}-\frac{b^2}{a^2}-2\log_e\frac{b}{a}$$

Formulation of the Heat Capacity Matrix.

The heat capacity term in equation (15) for i = A is

$$\frac{2\,P_m\,C_m}{2\Delta t}\int_{D^{(e)}}TN_A\;r\,dr\;\;d\theta$$

$$=\frac{P_m\,C_m}{\Delta t}\int_{D^{(e)}}\left[T_A\,N_A^2+T_B\,N_A\,N_B+T_C\,N_A\,N_C+T_D\,N_A\,N_D\right]r\,dr\;d\theta$$

In non-dimensional notation, the integrand becomes

$$T_A\frac{\left(\rho-\frac{b}{a}\right)^2(v-1)^2}{4\left(1-\frac{b}{a}\right)^2}+T_B\frac{\left(\rho-\frac{b}{a}\right)^2\left(v^2-1\right)}{-4\left(1-\frac{b}{a}\right)^2}$$

$$+T_C\frac{(\rho-1)\left(\rho-\frac{b}{a}\right)\left(v^2-1\right)}{4\left(1-\frac{b}{a}\right)^2}+T_D\frac{(\rho-1)\left(\rho-\frac{b}{a}\right)(v-1)^2}{-4\left(1-\frac{b}{a}\right)^2}$$

Now performing the integration over (ρ, ν) space

$$\frac{P_m\,C_m}{\Delta t}\int\left[\frac{\left(\rho-\frac{b}{a}\right)^2(v-1)^2}{4\left(1-\frac{b}{a}\right)^2}\right]a^2\,\alpha\rho\;d\rho\,dv$$

$$=\frac{P_m\,C_m\,a^2\,\alpha}{4q^2\,\Delta t}\int_{b/a}^{1}\rho\left(\rho-\frac{b}{a}\right)^2d\rho\int_{-1}^{1}(v-1)^2\,dv$$

$$=\frac{P_m\,C_m\,a^2\,\alpha}{36\,q^2\,\Delta t}[2D];\;[S_T]=\frac{P_m\,C_m\,a^2\,\alpha}{36\,q^2\,\Delta t}\begin{bmatrix}2D & D & -E & -2E\\ & 2D & -2E & -E\\ \text{SYM} & & 2F & F\\ & & & 2F\end{bmatrix}$$

Where,

$$D=3-8\frac{b}{a}+6\frac{b^2}{a^2}-\frac{b^4}{a^4};\quad E=-1+2\frac{b}{a}-2\frac{b^3}{a^3}+\frac{b^4}{a^4};$$

$$F=1-6\frac{b^2}{a^2}+8\frac{b^3}{a^3}-3\frac{b^4}{a^4}$$

Forcing Function Vector

From equation (15), the first term of the forcing function vector is:

$$\int_{D^{(e)}}QN_A\,r\,dr\,d\theta=\frac{Q}{2\left(\frac{b}{a}-1\right)}\int_{D^{(e)}}\left(\rho-\frac{b}{a}\right)(v-1)\left(a^2\,\alpha\,\rho\;d\rho\;dv\right)$$

$$=\frac{Qa^2\alpha}{\left(1-\frac{b}{a}\right)}\cdot\frac{1}{6}\left(2-3\frac{b}{a}+\frac{b^3}{a^3}\right)$$

Evaluating the other three, we obtain

$$[R]=\frac{Qa^2\alpha}{6q}\begin{bmatrix}G\\ G\\ H\\ H\end{bmatrix}$$

Where

$$G=2-3\frac{b}{a}+\frac{b^3}{a^3}\quad\text{and}\quad H=1-3\frac{b^2}{a^2}+2\frac{b^3}{a^3}$$

As a check, the sum of all these terms is Q α (a^2 - b^2), which is the total heat generated in the element.

Formulation of the heat convection matrix: On Cylindrical Curved Surface

The heat convection term in (15) for i = A is

$$\int_{S_2^{(e)}} h[N]\{T\}^{(e)} N_i \, ds_2$$

$$= h \int_{S_2^{(e)}} \left(T_A N_A^2 + T_B N_A N_B + T_C N_A N_C + T_D N_A N_D\right) ds_2$$

Now performing the integration in non-dimensional notation

$$h \int_{S_2^{(e)}} N_A^2 \, ds_2$$

$$= \frac{2}{3} h a \rho \infty \; ; \; h \int_{S_2^{(e)}} N_A N_B \, ds_2 = \frac{h a \rho \alpha}{3}$$

Evaluating the other terms, we obtain

$$[S_H] = h a \rho \alpha \begin{bmatrix} 2/3 & 1/3 & 0 & 0 \\ & 2/3 & 0 & 0 \\ \text{SYM} & & 0 & 0 \\ & & & 0 \end{bmatrix}$$

Heat Convection Vector: On cylindrical curved surface

From (15), the first term of the heat convection vector

$$\int_{S_2^{(e)}} h T_\infty N_A \, ds_2 = h T_\infty a \rho \alpha$$

Evaluating the other terms, we obtain

$$[s_T] = h T_\infty a \rho \alpha \begin{bmatrix} 1 \\ 1 \\ 0 \\ 0 \end{bmatrix}$$